Spheroidal harmonic expansions for the solution of Laplace's equation for a point source near a sphere

Matt R. A. Majić, Baptiste Auguié, and Eric C. Le Ru*
The MacDiarmid Institute for Advanced Materials and Nanotechnology, School of Chemical and Physical Sciences, Victoria University of Wellington, PO Box 600, Wellington 6140, New Zealand
(Received 4 October 2016; published 15 March 2017)

We propose a powerful approach to solve Laplace's equation for point sources near a spherical object. The central new idea is to use prolate spheroidal solid harmonics, which are separable solutions of Laplace's equation in spheroidal coordinates, instead of the more natural spherical solid harmonics. Using electrostatics as an example, we motivate this choice and show that the resulting series expansions converge much faster. This improvement is discussed in terms of the singularity of the solution and its analytic continuation. The benefits of this approach are further illustrated for a specific example: the calculation of modified decay rates of light emitters close to nanostructures in the quasistatic approximation. We expect the general approach to be applicable with similar benefits to the solution of Laplace's equation for other geometries and to other equations of mathematical physics.

DOI: 10.1103/PhysRevE.95.033307

I. INTRODUCTION

Laplace's equation is one of the most important partial differential equations of physics and engineering. It arises in many fields, including electromagnetism, classical gravity, and fluid dynamics. It also has close links, through the Laplacian operator, with other important differential equations of physics, such as the wave equation and the diffusion equation. Analytical solutions of Laplace's equation, typically obtained via the method of separation of variables, are standard materials for physics textbooks [1]. The solution for a point source located outside a sphere plays an especially important role through its connection with the Green's function formalism [2].

We will here focus on electrostatics, but our results extend to other applications of Laplace's equation. The standard electrostatics solution for a point source outside a dielectric sphere is relatively straightforward and obtained as a multipole expansion (infinite series) [2,3]. One important and often overlooked property of those series is that they can be very slowly convergent for sources close to the surface (often the most relevant situation), as shown explicitly in Ref. [4]. Moroz recently revisited this problem by focusing specifically on the decay rate of a dipole emitter near a sphere in the quasistatic approximation. This involved calculation of the reflected field at the dipole position (the self-field) and used mathematical manipulations to express the series solution in a more convergent form [5]. Lindell also approached this problem from the point of view of image theory where the outside potential is expressed as the potential of an "image" line charge inside the sphere [6], but the resulting solution involves an integral which must be computed numerically.

In this article, we propose and demonstrate an alternative approach based on the use of spheroidal harmonics, which are the separable solutions of Laplace's equation in spheroidal coordinates [1,2]. This choice may appear counterintuitive for a spherical object, but we will show that the spheroidal harmonics are better suited to the singularities of the solution. We show that the spheroidal harmonic series solution converges much faster than the standard spherical harmonic series. We show that this idea is also applicable to dipolar point sources of different orientations and derive new fast-converging series expansions for the quasistatic modified decay rates of emitters close to a sphere. We believe the applicability of this approach could extend to many other problems involving Laplace's equation, to other geometries, and to other equations of mathematical physics.

II. POINT CHARGE NEAR A DIELECTRIC SPHERE

To present our new approach, we will first focus on the simplest case of a point charge near a dielectric sphere. As illustrated in Fig. 1, we consider a point charge q located at $\mathbf{R}_P$, on the z axis at a distance d from a sphere of radius a ($|\mathbf{R}_P| = R_P = a + d$). The relative dielectric permittivities of the sphere and embedding medium are ϵ_2 and ϵ_1, respectively, and their ratio is denoted $\epsilon = \epsilon_2/\epsilon_1$ for convenience. Our results will be illustrated for a dielectric sphere with $\epsilon = 2.25$, but similar conclusions are obtained for other values of ϵ. The results are scale invariant; i.e., they only depend on d/a, and we are particularly interested in situations where $d/a \ll 1$.

We seek the outside potential $V(\mathbf{r})$, solution of Laplace's equation in the presence of this point charge. For convenience, we write $V = \bar{V} q/(4\pi\epsilon_0\epsilon_1 a)$ and work with the dimensionless $\bar{V}$. The standard solution of this problem consists in expanding the point charge potential $\bar{V}_q$ as a series of regular solid harmonics centered on the sphere [2],

$$\bar{V}_q = \frac{a}{R_P}\sum_{n=0}^{\infty}\left(\frac{r}{R_P}\right)^n P_n(\cos\theta) \quad (r < R_P), \tag{1}$$

where (r,θ,ϕ) are spherical coordinates and P_n are the Legendre polynomials. The potential outside the sphere ($r > a$) is written as $\bar{V}_{\text{out}} = \bar{V}_q + \bar{V}_r$. The "reflected" potential $\bar{V}_r$ can be derived by assuming a spherical solid harmonic expansion and

*eric.leru@vuw.ac.nz

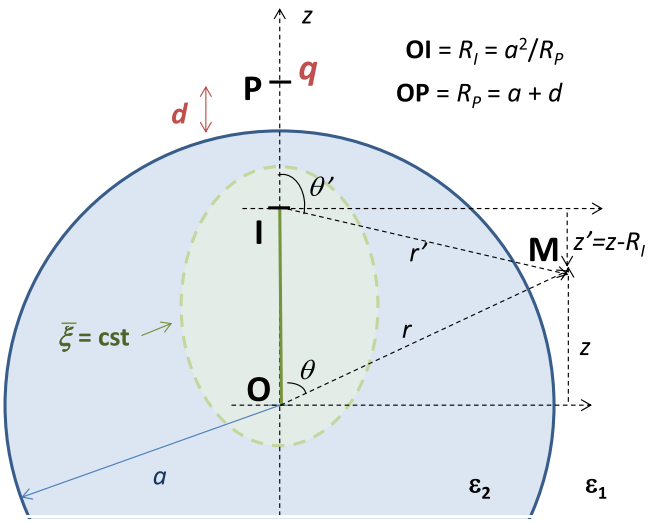

FIG. 1. Schematic of the electrostatics problem under study: a point charge q at a distance d from a sphere of radius a. The various coordinate systems used in the solution are also illustrated: spherical (r,θ,ϕ), offset spherical (r',θ',ϕ), and offset prolate spheroidal $(\bar{\xi},\bar{\eta},\phi)$.

applying electrostatic boundary conditions on the surface [2],

$$\bar{V}_r = -\sum_{n=0}^{\infty} \beta_n \left(\frac{R_I}{r}\right)^{n+1} P_n(\cos\theta), \tag{2}$$

where $R_I = a^2/R_P$ and the adimensional sphere polarizabilities are

$$\beta_n = \frac{n(\epsilon-1)}{n(\epsilon+1)+1}. \tag{3}$$

We also define $\beta_\infty = (\epsilon-1)/(\epsilon+1)$, which is related to the response of a planar interface.[1]

As discussed in Refs. [4–6], the sum in Eq. (2) can be very slowly convergent when evaluated at or in the vicinity of the sphere surface ($r \approx a$) for a point source close to the sphere ($d \ll a$). The rate of convergence can be studied by considering the the relative error e_N in the partial series (truncated at N terms) with respect to its converged value (computed with enough terms to ensure it no longer depends on the number of terms within double floating point precision), explicitly for a general series $\sum_n t_n$:

$$e_N = \left| 1 - \sum_{n=0}^{N} t_n \Big/ \sum_{n=0}^{\infty} t_n \right|. \tag{4}$$

This is shown explicitly in Fig. 2 for the series in Eq. (2) for the potential at different points close to or on the sphere surface. For example, one needs to sum more than 1500 terms in the series to obtain a converged solution (within the double-precision accuracy of $\sim 10^{-15}$) of the potential on the sphere surface when $d/a = 0.02$. This slow convergence also occurs everywhere on the sphere surface, not just in the vicinity of the point source.

In order to motivate our choice of working with prolate spheroidal coordinates, we first derive a faster converging formulation of the solution with spherical coordinates, where the nature of the singularities of the solution becomes more apparent. For this, we start from Eq. (2) and isolate the dominant contribution for large n by writing

$$\beta_n = \beta_\infty - \frac{\beta_\infty}{n(\epsilon+1)+1}. \tag{5}$$

Substituting back into Eq. (2), the second term gives a series that converges faster and the first term gives a series for which we recognize a closed-form analytical expression:[2]

$$-\beta_\infty \sum_{n=0}^{\infty} \left(\frac{R_I}{r}\right)^{n+1} P_n(\cos\theta) = -\frac{\beta_\infty R_I}{|\mathbf{r} - R_I\hat{\mathbf{z}}|}. \tag{6}$$

This can be viewed as the potential created by an image point charge $q_I = -q\beta_\infty(R_I/a)$, located at a distance R_I from the origin on the z axis (point I; see Fig. 1). This is the same image charge location as that used in the method of images to solve the same problem for a perfect conductor [2,7]. The solution then takes the form (the primed coordinates refer to those centered at I):

$$\bar{V}_r = -\beta_\infty \frac{R_I}{r'} + \sum_{n=0}^{\infty} \frac{\beta_\infty}{n(\epsilon+1)+1} \left(\frac{R_I}{r}\right)^{n+1} P_n(\cos\theta). \tag{7}$$

The slow convergence of the series in Eq. (2) has been partially removed by isolating and recognizing the analytical expression for the image charge. Nevertheless, the convergence of the series in Eq. (7) remains slow (Fig. 3). This approach can be repeated to further improve the convergence. Isolating the next term and recognizing its closed-form expression, we obtain after manipulation (see Appendix A)

$$\bar{V}_r = -\beta_\infty \frac{R_I}{r'} + \frac{\beta_\infty}{\epsilon+1} \ln\frac{r'-z'}{r-z} + \frac{\epsilon\beta_\infty}{\epsilon+1} \sum_{n=0}^{\infty} \left(\frac{R_I}{r}\right)^{n+1} \frac{P_n(\cos\theta)}{(n+1)[n(\epsilon+1)+1]}. \tag{8}$$

As shown in Fig. 3, the convergence of Eq. (8) is again improved, but still requires a large number of terms (~800) to

[1] For a point charge near a planar interface, the reflected potential is simply that of an image point charge located at the mirror image position (with respect to the plane) and of amplitude $q' = -\beta_\infty q$. The solution for the sphere reduces to that of the plane in the limit $d/a \to 0$, but even for $d/a = 0.02$, the sphere and plane solutions still differ by ~10%.

[2] Equation (6) may be recognized as the expression for translation of solid spherical harmonics along the z axis [2,7] and can be proved using the generating function of the Legendre polynomials [8].

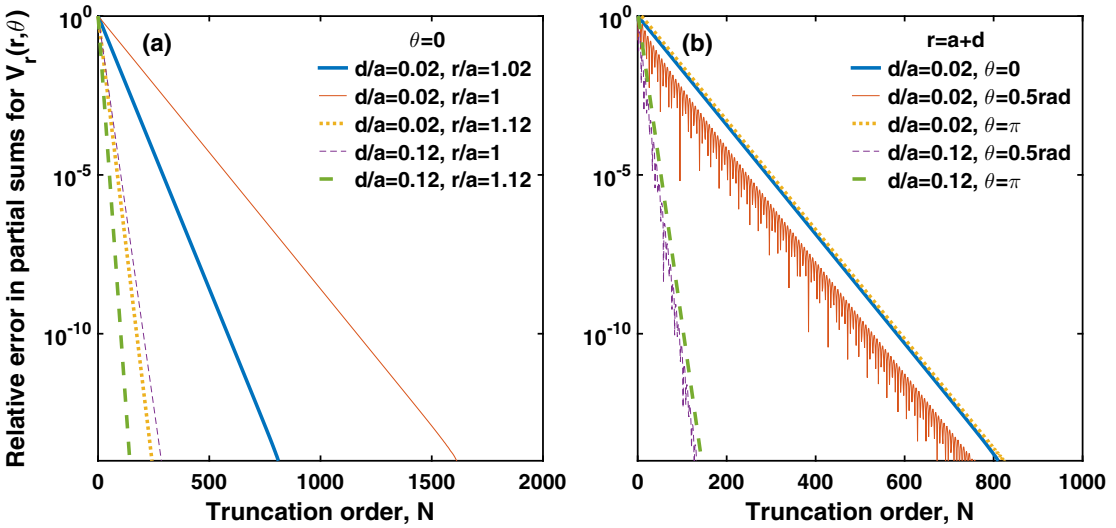

FIG. 2. Convergence of the standard series solution [Eq. (2)] for a point charge at a distance of $d = 0.02a$ or $d = 0.12a$ from a dielectric sphere of radius a (with $\epsilon = 2.25$). Note that the results are scale independent. Relative errors in the partial sums are computed by comparing the series with N terms to the same series with enough terms to have converged to double floating point precision (i.e., accurate to within $\sim 10^{-15}$). Errors are shown for the outside potential at different positions either along the z axis (a) or off axis for $r = a + d$ (b). The noisy appearance of the off-axis errors is due to the oscillations of the Legendre polynomials when $\cos\theta \neq 1$.

reach double-precision accuracy. It is also interesting to note that the second term in Eq. (8) exhibits a singularity on the line segment OI; this term can be viewed as the potential of an extended image source over this segment. In fact, the solution of the problem within the method of images was previously found to give [6]

$$\bar{V}_r = -\beta_\infty \frac{R_I}{r'} + \frac{\beta_\infty}{\epsilon+1}\int_0^{R_I} \frac{(\tilde{z}/R_I)^{\epsilon/(\epsilon+1)} d\tilde{z}}{\sqrt{x^2+y^2+(z-\tilde{z})^2}}, \tag{9}$$

from which a line image charge over OI is also evident. This extended line singularity found in both approaches provides the motivation for our proposed new approach to the problem.

III. SPHEROIDAL HARMONIC SOLUTION

Instead of using a spherical harmonics expansion, we search for a solution in a basis of spheroidal harmonics, namely,

$$\bar{V}_r = \sum_{n=0}^{\infty} a_n Q_n(\bar{\xi}) P_n(\bar{\eta}). \tag{10}$$

$Q_n(\bar{\xi})P_n(\bar{\eta})$ are irregular solid prolate spheroidal harmonics; i.e., they are the standard separable solutions of Laplace's equation (where there is no ϕ dependence) in prolate spheroidal coordinates, with $Q_n(\bar{\xi})$ the Legendre functions of the second kind (see Appendix B for definition). $\bar{\xi}$ and $\bar{\eta}$ are prolate spheroidal coordinates *with focal points at O, center of sphere, and I, position of the image charge*. Explicitly, $\bar{\xi}$ and $\bar{\eta}$ are

$$\bar{\xi} = \frac{r+r'}{R_I}, \quad \bar{\eta} = \frac{r-r'}{R_I}. \tag{11}$$

The "bar" notation is used here to emphasize the fact that prolate spheroidal coordinates are traditionally defined differently with O at the midpoint between the two foci [1]. We choose these coordinates because $Q_n(\bar{\xi})$ is then singular exactly on the segment OI ($\bar{\xi} = 1$), where the singularity of the solution occurs.

To determine the expansion coefficients a_n, we first need to find the expansion for the irregular spherical solid harmonics $P_n(\cos\theta)/r^{n+1}$ in terms of the irregular prolate spheroidal solid harmonics. Such expansions can be found in the literature [9,10] in the case where the spherical harmonics center is in the middle of the focal points used for the spheroidal coordinates. In our case, however, the sphere center corresponds to one of the focal points, so a new expression had to be derived. The details are provided in Appendix C and we here state the final result:

$$\left(\frac{R_I}{r}\right)^{n+1} P_n(\cos\theta) = \sum_{k=n}^{\infty} (-1)^{n+k} \frac{2(2k+1)(k+n)!}{n!^2(k-n)!} Q_k(\bar{\xi}) P_k(\bar{\eta}). \tag{12}$$

One can then substitute this expansion into the original solution [Eq. (2)], swap the order of the sums, and relabel the indices $n \leftrightarrow k$, to obtain the coefficients a_n as

$$a_n = -2(2n+1)\sum_{k=1}^{n} (-1)^{n+k} \frac{(n+k)!}{k!^2(n-k)!}\beta_k. \tag{13}$$

For the problem at hand, it is actually beneficial to first isolate the point singularity (image charge) identified earlier, since it does not exhibit the same line singularity as found in the spheroidal solid harmonics. We therefore look for a solution of the form

$$\bar{V}_r = -\beta_\infty \frac{R_I}{r'} + \sum_{n=0}^{\infty} b_n Q_n(\bar{\xi}) P_n(\bar{\eta}). \tag{14}$$

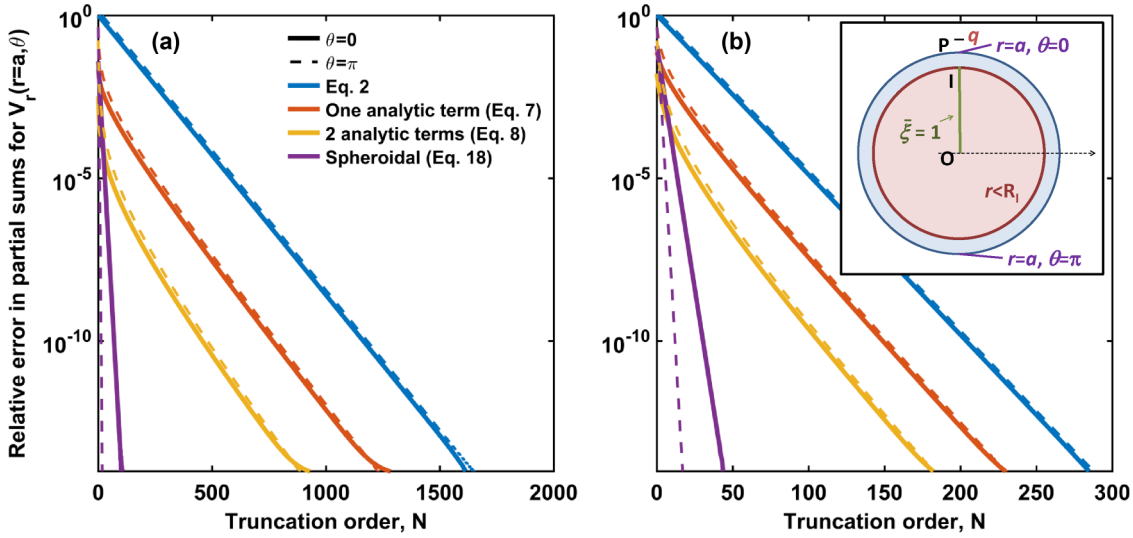

FIG. 3. Convergence of the improved series solutions for the outside potential at the surface ($r = a$) either close to the source ($\theta = 0$, solid lines) or at the opposite side of the sphere ($\theta = \pi$, dashed lines) for a point charge at a distance $d = 0.02a$ (a) or $d = 0.12a$ (b). We compare the standard solution [Eq. (2)] with the improved solutions with the image charge term [Eq. (7)] and with the logarithmic term [Eq. (8)]. The new approach using a spheroidal harmonics expansion [Eq. (18)] is also compared to those and converges much faster, especially for sources very close to the sphere. The inset in (b) depicts the region of divergence of the series for spherical (inside circle in red) and spheroidal (segment OI in green) harmonics expansions.

As for a_n, the coefficients b_n are obtained by substituting Eq. (12) into the series in Eq. (7) and swapping the order of the sums. We obtain

$$b_n = \beta_\infty 2(2n+1)c_n, \tag{15}$$

$$\text{with} \quad c_n = \sum_{k=0}^{n} \frac{(-1)^{n+k}}{k(\epsilon+1)+1} \frac{(n+k)!}{k!^2(n-k)!}. \tag{16}$$

This expression is, however, not suitable for practical computations as large numerical errors appear in the sum at relatively low n ($\approx$20), but one can derive the following equivalent expression (see Appendix D):

$$c_n = \prod_{k=0}^{n} \frac{\mu - k}{\mu + k}, \quad \text{where } \mu = \frac{1}{\epsilon + 1}. \tag{17}$$

With this expression, c_n can be computed easily by recurrence. The reflected potential is then

$$\bar{V}_r = -\beta_\infty \frac{R_I}{r'} + \beta_\infty \sum_{n=0}^{\infty} 2(2n+1)c_n Q_n(\bar{\xi}) P_n(\bar{\eta}). \tag{18}$$

The convergence of this series is compared in Fig. 3 to those previously obtained, and the improvements are dramatic. It should be noted that care should be taken in the computation of the Legendre functions of the second kind, which were computed using a backward recurrence and the modified Lentz algorithm [11]. In the example of Fig. 3(a), where $d/a = 0.02$, full accuracy is obtained for the surface potential close to the point source with only $\sim$100 terms instead of $\sim$1600 for the standard solution. The benefits are even more dramatic elsewhere on the surface, with only 20 terms needed on the other side of the sphere. The results of Fig. 3 were also reproduced (not shown here) for many different values of ϵ, including complex-valued, and almost identical graphs were obtained for all of them.

To understand these improvements, we recognize that Eq. (18) provides an analytic continuation of Eq. (8). Those infinite series are strictly equivalent in the region where they both converge, but their ranges of convergence are different: Eq. (8) converges only for $r > R_I$, while Eq. (18) converges everywhere except on the segment OI. One naturally expects that slow convergence of either series will occur near the boundary of its region of convergence. For spheroidal expansions, the point $r = R_P$, $\theta = \pi$ is far from the segment of divergence OI [see inset in Fig. 3(b)], and the series therefore converges rapidly. For spherical expansions, this point is very close to the sphere of divergence, and convergence is very slow. The logarithmic term in Eq. (8) and previous studies using the method of images [6] suggest that the analytic continuation of the solution is singular only on the segment OI and the divergence region cannot be further reduced. This suggests that the spheroidal solid harmonics (centered on the segment OI) are the most natural basis for this problem, which explains the faster convergence even at points near the singularity at I.

IV. POINT DIPOLE AND MODIFIED DECAY RATES IN THE QUASISTATIC APPROXIMATION

To illustrate the usefulness of the proposed method, we now discuss an application that is relevant to current areas of research involving emitters on nanoparticles, including nanophotonics, plasmonics, and surface-enhanced spectroscopy [4]. For a nanostructure that is much smaller than the light wavelength, its optical response is well described by a quasistatic approximation, which consists in solving the corresponding electrostatics problem (i.e., taking the limit of a vanishing wave number in Helmholtz' equation, which reduces to Laplace's equation), but still using the material's

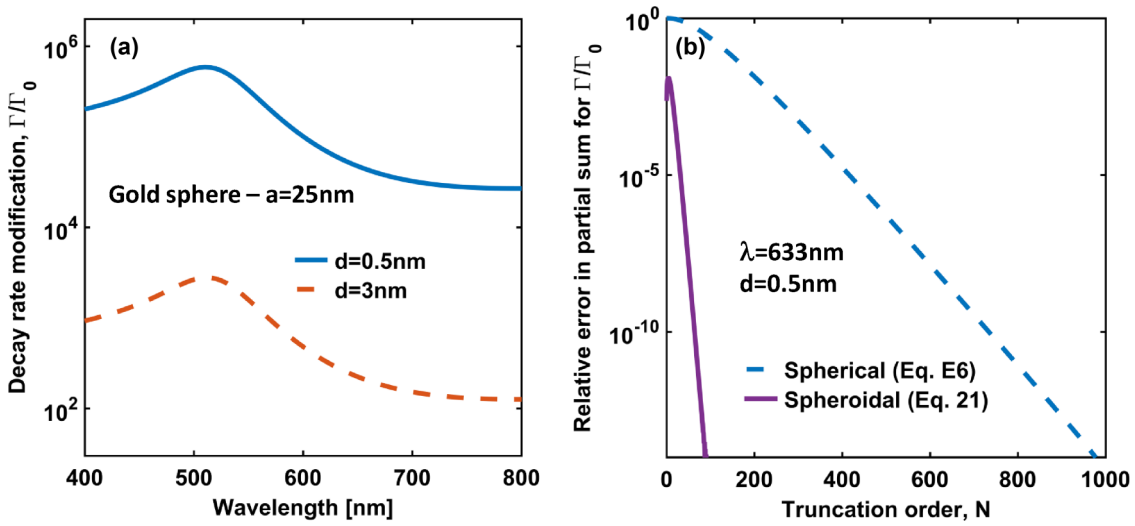

FIG. 4. (a) Spectral variation of the decay rate modification in the electrostatics approximation for a dipole perpendicular to a gold sphere of radius $a = 25$ nm embedded in water ($\epsilon_1 = 1.33^2$), at a distance $d = 0.5$ or 3 nm from the surface. The dielectric function for gold is taken from Ref. [17]. (b) Convergence of the standard and improved series solutions for the modified decay rates $\Gamma_\perp/\Gamma_0$ at wavelength $\lambda = 633$ nm (where $\epsilon = -6.5 + 0.67i$) and $d = 0.5$ nm (i.e., $d/a = 0.02$). The spheroidal expansion [Eq. (21)] requires much fewer terms for accurate results. Almost identical results are obtained for the parallel dipole (not shown).

dielectric function corresponding to the optical frequency. The electrostatic solution for a point dipole near a dielectric or metallic object can be used to calculate the modified decay rate of a single emitter near a nanoparticle. A number of recent studies have been dedicated to this aspect [12,13]. In this section, we show how the new approach can be used in this context to obtain new series expressions for the quasistatic modified decay rates near a sphere, which converge much faster than those proposed to date [5].

We consider a dipole $\mathbf{p}$ located at a distance d from the sphere on the z axis. The dimensionless potential $\bar{V}$ is now defined as $V = \bar{V}\, p/(4\pi\epsilon_0\epsilon_1 a R_P)$ (where $p = |\mathbf{p}|$) for convenience. For a perpendicular dipole (oriented along z), the reflected potential can be expressed using solid spheroidal harmonics expansions as (see Appendix E for details)

$$\bar{V}_\perp = \beta_\infty \frac{R_I^2 z'}{r'^3} + \frac{\epsilon\beta_\infty}{\epsilon+1}\frac{R_I}{r'} - \frac{\epsilon\beta_\infty}{\epsilon+1}\sum_{n=0}^{\infty} 2(2n+1)c_n Q_n(\bar{\xi})P_n(\bar{\eta}). \tag{19}$$

The first two terms correspond to an image dipole and image point charge, respectively, while the series exhibit a line singularity over the segment OI as before.

The modified decay rate Γ for a dipolar emitter can be deduced from its self-field $\mathbf{E}_{\rm sf}$ as [3,4,14–16]

$$\frac{\Gamma}{\Gamma_0} = 1 + \frac{6\pi\epsilon_0\epsilon_1}{k_1^3}\frac{\mathrm{Im}(\mathbf{p}^*\cdot\mathbf{E}_{\rm sf})}{|\mathbf{p}|^2}, \tag{20}$$

where Γ_0 is the normal decay rate in the embedding medium, $k_1 = (2\pi/\lambda)\sqrt{\epsilon_1}$ is the wave-number, and $\mathbf{E}_{\rm sf}$ is the electric field at the dipole position resulting from the presence of the sphere nearby. In the quasistatic approximation, valid for spheres much smaller than the wavelength, the field solution close to the sphere can be approximated by the corresponding electrostatics solution using the wavelength-dependent dielectric function (which may be complex). The self-field $\mathbf{E}_{\rm sf}$ can then be obtained by evaluating the reflected field $\mathbf{E}_r = -\nabla V_r$ at the dipole position. For a dipole that is either perpendicular ($\perp$) or parallel ($\parallel$) to the sphere, we obtain (see Appendixes E and F)

$$\frac{\Gamma_\perp}{\Gamma_0} = 1 + \frac{3}{2(k_1 a)^3}\mathrm{Im}\left[\beta_\infty\left(\frac{2}{\delta_P^3} + \frac{\epsilon}{\epsilon+1}\frac{1}{\delta_P^2}\left\{1 - \frac{1}{\delta_P(1+\delta_P)}\sum_{n=0}^{\infty}(2n+1)(n+1)c_n[\bar{\xi}_P Q_n(\bar{\xi}_P) - Q_{n+1}(\bar{\xi}_P)]\right\}\right)\right],$$
$$\frac{\Gamma_\parallel}{\Gamma_0} = 1 - \frac{3}{2(k_1 a)^3}\mathrm{Im}\left\{\beta_\infty\left[\frac{1}{\delta_P^3} - \frac{2}{\epsilon+1}\frac{1}{\sqrt{\delta_P(1+\delta_P)}}\sum_{n=1}^{\infty}(2n+1)(c_n-1)Q_n^1(\bar{\xi}_P)\right]\right\}. \tag{21}$$

where we have defined $\delta_P = (R_P/a)^2 - 1$ ($\delta_P \ll 1$ when the dipole is close to the surface), $\bar{\xi}_P = 1 + 2\delta_P$, and Q_n^m are the associated Legendre functions of the second kind. Note that β_∞ and the coefficients c_n in the series depend on ϵ and may be complex; they contribute to the material dependence of the whole expression. As an example, we consider a 25-nm-radius gold nanosphere in water. Figure 4(a) shows the wavelength dependence of the modified decay rate for a perpendicular dipole at a distance $d = 0.5$ and 3 nm from the surface. The convergence of the new formula [Eq. (21)] is also compared in Fig. 4(b) to that of the standard expression obtained from spherical harmonics expansions [4,5]. Much

faster convergence is seen, highlighting again the benefits of the approach.

V. CONCLUSION AND OUTLOOK

Using electrostatics as an example, we have shown that spheroidal harmonics expansions are better suited than spherical harmonics to solving Laplace's equation in the presence of point sources located close to spherical boundaries. This counterintuitive conclusion can be understood when considering that the singularity of the solution occurs on a line segment in such problems. A judicious choice of spheroidal solid harmonics ensures that the basis functions in the expansion have a singularity matching the one of the solution. This is not possible with spherical solid harmonics, which all exhibit a point rather than segment singularity.

This argument indicates that our proposed approach would be applicable to many related problems. We have here considered point charges and point dipoles in electrostatics, and higher-order multipole point sources near a sphere could be studied with minor modifications. Beyond those examples, the method could be adapted to study the potential solution inside the sphere, problems with different boundary conditions on the sphere surface, and similar problems in other fields using Laplace's equation. Spheroidal harmonics expansions could also provide new approaches to solve Laplace's equation with other geometries, for example, interacting spheres (where one sphere can be viewed as a source for the other) or of a sphere near an infinite plane. We also envisage that our arguments could be extended to other equations of mathematical physics, such as the Helmholtz equation. The full-wave series solution for a dipole near a sphere is also slowly convergent but the problem becomes more acute because numerical problems arise in computing those series for large n; the terms in the series include spherical Bessel functions of $k_1 r$ whose values can commonly reach beyond double-precision arithmetic at large orders. The solutions cannot therefore be easily computed numerically for dipoles close to the sphere. Spheroidal harmonics expansions (which may involve the standard spheroidal wave functions [18] or alternative definitions) may alleviate such issues. Although all those extensions will require further developments, the results presented in this article provide a vivid demonstration of the usefulness of spheroidal coordinates in problems with symmetry of revolution where they may have been overlooked so far.

APPENDIX A: PROOF OF EQ. (8), CLOSED-FORM EXPRESSION FOR LOGARITHMIC TERM

The same approach as carried out to find the image charge term [Eq. (7)] can be followed to obtain the next dominant term. We isolate the next dominant term in β_n by writing

$$\frac{n}{n(\epsilon+1)+1} = \frac{1}{\epsilon+1} - \frac{1}{(\epsilon+1)^2}\frac{1}{n+1} - \frac{\epsilon}{(\epsilon+1)^2}\frac{1}{(n+1)[n(\epsilon+1)+1]}. \quad \text{(A1)}$$

The choice of factor $1/(n+1)$ in the second term, instead of for example $1/n$, may look arbitrary but will simplify the calculations. When substituting back Eq. (A1) into Eq. (2), the first term gives the same image charge term as found in Eq. (7). The analytic expression for the sum over the second term in Eq. (A1) is less obvious. It involves the series

$$\sum_{n=0}^{\infty}\left(\frac{R_I}{r}\right)^{n+1}\frac{P_n(\cos\theta)}{n+1}. \quad \text{(A2)}$$

To calculate it, we start from the generating function of the Legendre polynomials:

$$\frac{1}{\sqrt{1-2xt+t^2}} = \sum_{n=0}^{\infty} t^n P_n(x), \quad (|t|<1). \quad \text{(A3)}$$

Integrating with respect to t,

$$\ln\left|\frac{t-x+\sqrt{1-2xt+t^2}}{1-x}\right| = \sum_{n=0}^{\infty}\frac{t^{n+1}}{n+1}P_n(x), \quad \text{(A4)}$$

for $|t|<1$. Setting $x=\cos\theta$ and $t=R_I/r$, we obtain, after simplifications,

$$\sum_{n=0}^{\infty}\left(\frac{R_I}{r}\right)^{n+1}\frac{P_n(\cos\theta)}{n+1} = \ln\frac{r'-z'}{r-z} \quad (r>R_I), \quad \text{(A5)}$$

where primed coordinates refer to the coordinates in the frame centered on point I:

$$\begin{aligned} &\rho' = \rho = r\sin\theta, \quad z' = z - R_I, \\ &r' = \sqrt{\rho^2+(z-R_I)^2}, \quad \theta' = \cos^{-1}\frac{z'}{r'}. \end{aligned} \quad \text{(A6)}$$

Equation (8) then follows for $r>R_I$ by substituting Eq. (A1) into Eq. (2) and using the analytic forms of the series given in Eqs. (6) and (A5).

It is also interesting to note that the logarithmic term found here is directly related to the prolate solid spheroidal harmonic for $n=0$:

$$Q_0(\bar{\xi})P_0(\bar{\eta}) = \frac{1}{2}\ln\frac{\bar{\xi}+1}{\bar{\xi}-1} = \frac{1}{2}\ln\frac{r'-z'}{r-z}. \quad \text{(A7)}$$

The latter equality is not obvious but can be proved by inverting the definitions of $\bar{\xi}$ and $\bar{\eta}$:

$$\begin{aligned} &r = \frac{R_I}{2}(\bar{\xi}+\bar{\eta}); \quad r' = \frac{R_I}{2}(\bar{\xi}-\bar{\eta}); \\ &z = \frac{R_I}{2}(\bar{\xi}\bar{\eta}+1); \quad z' = \frac{R_I}{2}(\bar{\xi}\bar{\eta}-1). \end{aligned} \quad \text{(A8)}$$

Then we have

$$\frac{r'-z'}{r-z} = \frac{(\bar{\xi}-\bar{\eta})-(\bar{\xi}\bar{\eta}-1)}{(\bar{\xi}+\bar{\eta})-(\bar{\xi}\bar{\eta}+1)} = \frac{(\bar{\xi}+1)(\bar{\eta}-1)}{(\bar{\xi}-1)(\bar{\eta}-1)} = \frac{\bar{\xi}+1}{\bar{\xi}-1}. \quad \text{(A9)}$$

This link [Eq. (A7)] provides further motivation for the use of spheroidal solid harmonics expansions.

APPENDIX B: DEFINITION AND COMPUTATION OF THE LEGENDRE FUNCTIONS OF THE FIRST AND SECOND KINDS

The associated Legendre functions of the first kind are widely used, but there are different conventions. We used the

following definition (for $m \geqslant 0$ and $x \in \mathbb{R}$):

$$P_n^m(x) = |x^2-1|^{m/2}\frac{d^m P_n(x)}{dx^m}. \tag{B1}$$

Note that it is common to add an extra $(-1)^m$ to this definition when $|x| \leqslant 1$, for example, when $x = \cos\theta$ for the definition of spherical harmonics [7]. Our convention is arguably more convenient when also considering $x > 1$, which is the case when working with the regular solid spheroidal harmonics [which contain $P_n^m(\xi)$].

The $P_n^m(x)$ are computed by forward recurrence on n (for a fixed m) using the relation

$$(n-m+1)P_{n+1}^m = (2n+1)xP_n^m - (n+m)P_{n-1}^m, \tag{B2}$$

and the initial conditions

$$\begin{aligned} P_m^m(x) &= (2m-1)!!|1-x^2|^{m/2}, \\ P_{m+1}^m(x) &= (2m+1)xP_m^m(x). \end{aligned} \tag{B3}$$

The associated Legendre functions of the second kind are much less common. They are defined as follows for $x \in \mathbb{R}$ [9]. For $m = 0$, we have

$$Q_0(x) = \frac{1}{2}\ln\left|\frac{x+1}{x-1}\right|, \quad Q_1(x) = xQ_0(x) - 1, \tag{B4}$$

and as for the Legendre polynomials,

$$(n+1)Q_{n+1} = (2n+1)xQ_n - nQ_{n-1}. \tag{B5}$$

However, stable computation of $Q_n(x)$ is more complicated as this simple forward recurrence becomes quickly numerically unstable as n increases. Instead, we have therefore used a stable backward recurrence described in Ref. [11], which is based on the modified Lentz algorithm.

For $m > 0$, similarly to the functions of the first kind, we have

$$Q_n^m(x) = |x^2-1|^{m/2}\frac{d^m Q_n(x)}{dx^m}, \tag{B6}$$

and Q_n^m obeys exactly the same recurrence as in Eq. (B2). Note also that P_n^1 and Q_n^1 can be easily derived from the $m = 0$ functions from

$$\begin{matrix} Q_n^1 \\ P_n^1 \end{matrix}(x) = \frac{n}{\sqrt{|x^2-1|}}\left[x\begin{matrix} Q_n \\ P_n \end{matrix}(x) - \begin{matrix} Q_{n-1} \\ P_{n-1} \end{matrix}(x)\right] \quad (n \geqslant 1). \tag{B7}$$

APPENDIX C: EXPANSION OF SPHERICAL SOLID HARMONICS IN TERMS OF SPHEROIDAL SOLID HARMONICS

Such expansions can be found in the literature [9,10] in the case where the spherical harmonics center is in the middle of the focal points used for the spheroidal coordinates. There are four main formulas, corresponding to the expansion of regular (irregular) spherical solid harmonics in terms of regular (irregular) spheroidal harmonics and vice versa. Two of them are reproduced below [9,10],

$$P_n^m(\xi)P_n^m(\eta) = \sum_{\substack{k=m \\ n+k \text{ even}}}^{n} \frac{(-)^{(n-k)/2}(n+k-1)!!}{(n-k)!!(k+m)!} \times \frac{(n+m)!}{(n-m)!}\left(\frac{r}{c}\right)^k P_k^m(\cos\theta), \tag{C1}$$

$$\left(\frac{c}{r}\right)^{n+1} P_n^m(\cos\theta) = \sum_{\substack{k=n \\ n+k \text{ even}}}^{\infty} (-)^{(n-k)/2+m}(2k+1) \times \frac{(n+k-1)!!}{(k-n)!!(n-m)!}\frac{(k-m)!}{(k+m)!}Q_k^m(\xi)P_k^m(\eta), \tag{C2}$$

where $(-)^n$ is shorthand for $(-1)^n$. The foci are located at $z = \pm c$ on the z axis and the prolate spheroidal coordinates for those focal points are given by (we use the definition of Ref. [1])

$$\begin{aligned} \xi &= \frac{\sqrt{r^2+2cz+r^2} + \sqrt{r^2-2cz+r^2}}{2c}, \\ \eta &= \frac{\sqrt{r^2+2cz+r^2} - \sqrt{r^2-2cz+r^2}}{2c}. \end{aligned}$$

In our case, however, the sphere center corresponds to one of the focal points, and the other one is a $z = R_I$, so the spheroidal coordinates are given as

$$\bar{\xi} = \frac{r+\sqrt{r^2-2zc+c^2}}{c}, \quad \bar{\eta} = \frac{r-\sqrt{r^2-2zc+c^2}}{c},$$

with $c \equiv R_I$. We therefore derived new expansions between spherical and the corresponding offset spheroidal harmonics:

$$P_n^m(\bar{\xi})P_n^m(\bar{\eta}) = \frac{(n+m)!}{(n-m)!}\sum_{k=m}^{n}\frac{(-)^{n+k}}{k!(k+m)!} \times \frac{(n+k)!}{(n-k)!}\left(\frac{r}{c}\right)^k P_k^m(\cos\theta), \tag{C3}$$

$$\left(\frac{c}{r}\right)^{n+1} P_n^m(\cos\theta) = \frac{2}{n!(n-m)!}\sum_{k=n}^{\infty}(-)^{n+k+m}(2k+1) \times \frac{(k+n)!}{(k-n)!}\frac{(k-m)!}{(k+m)!}Q_k^m(\bar{\xi})P_k^m(\bar{\eta}). \tag{C4}$$

The relation we use in Sec. III [Eq. (12)] is Eq. (C4), with $c \equiv R_I$ and $m = 0$. Equation (C3) will be needed here only in the proof of Eq. (C4).

Proof of Eq. (C3). Consider the expansion of regular solid prolate harmonics $P_n^m(\bar{\xi})P_n^m(\bar{\eta})\exp(im\phi)$ in terms of regular solid spherical harmonics $r^k P_k^m(\cos\theta)\exp(im\phi)$, which must exist since the solid harmonics are a basis for regular solutions to Laplace's equation. We can assume the m are the same on both sides since ϕ is the same in both coordinate systems and $\exp(im\phi)$ are independent functions. So we write

$$P_n^m(\bar{\xi})P_n^m(\bar{\eta}) = \sum_{k=0}^{\infty}\alpha_{nk}^m\left(\frac{r}{c}\right)^k P_k^m(\cos\theta). \tag{C5}$$

The associated Legendre functions (see definitions in Appendix B) can be written as

$$P_n^m(x) = |1-x^2|^{m/2}\Pi_n^m(x),$$
$$\text{where} \quad \Pi_n^m(x) = \frac{d^m}{dx^m}P_n(x). \tag{C6}$$

Using the relation

$$(1-\bar{\eta}^2)(\bar{\xi}^2-1) = \frac{4r^2}{c^2}\sin^2\theta, \tag{C7}$$

we deduce

$$P_n^m(\bar{\xi})P_n^m(\bar{\eta}) = \left(\frac{2r}{c}\right)^m \sin^m\theta\,\Pi_n^m(\bar{\xi})\Pi_n^m(\bar{\eta}). \tag{C8}$$

Equation (C5) can therefore be written in terms of Π_n^m as

$$\Pi_n^m(\bar{\xi})\Pi_n^m(\bar{\eta}) = \sum_{k=m}^{\infty}\alpha_{nk}^m\left(\frac{r}{c}\right)^{k-m}\frac{1}{2^m}\Pi_k^m(\cos\theta). \tag{C9}$$

The coefficients α_{nk}^m can be determined by evaluating the expansion for $\theta = 0$ and $r > c, z > c$, which implies $\bar{\eta} = 1$ and $r = c(\bar{\xi}+1)/2$. Using the special value

$$\Pi_n^m(1) = \frac{1}{2^m}\frac{(n+m)!}{m!(n-m)!}, \tag{C10}$$

we obtain

$$\Pi_n^m(\bar{\xi}) = \sum_{k=0}^{\infty}\alpha_{nk}^m\frac{(k+m)!(n-m)!}{(k-m)!(n+m)!}\frac{1}{2^m}\left(\frac{\bar{\xi}+1}{2}\right)^{k-m}. \tag{C11}$$

We then use the following identity for the Legendre polynomials:

$$P_n(x) = \sum_{k=0}^{n}(-)^{n+k}\frac{(n+k)!}{k!^2(n-k)!}\left(\frac{x+1}{2}\right)^k. \tag{C12}$$

By differentiating m times with respect to x, we get

$$\Pi_n^m(x) = \sum_{k=m}^{n}\frac{(-)^{n+k}k!}{2^m(k-m)!}\frac{(n+k)!}{k!^2(n-k)!}\left(\frac{x+1}{2}\right)^{k-m}. \tag{C13}$$

From this and Eq. (C11), we identify

$$\alpha_{nk}^m = \frac{(n+m)!}{(n-m)!}(-)^{n+k}\frac{(n+k)!}{k!(n-k)!(k+m)!} \tag{C14}$$
$$\text{for} \quad m \leqslant k \leqslant n, \quad 0 \text{ otherwise},$$

which proves Eq. (C3). Note that since the expansion is finite, it converges everywhere and is valid in all space. ■

Proof of Eq. (C4). To prove Eq. (C4), we will make use of the expansions of Green's function in terms of both spherical and spheroidal solid harmonics. The expansion in terms of spheroidal harmonics can be found, for example, in Ref. [9] for standard prolate spheroidal coordinates and it can be adapted to our modified coordinates with a simple scaling factor of 2, which comes from shrinking the focal length of the coordinates from $2c$ to c. For two points $\mathbf{r}_1$ and $\mathbf{r}_2$ with spheroidal coordinates denoted $(\bar{\xi}_1,\bar{\eta}_1,\phi_1)$ and $(\bar{\xi}_2,\bar{\eta}_2,\phi_2)$, we have when $\bar{\xi}_1 < \bar{\xi}_2$

$$\frac{1}{|\mathbf{r}_1-\mathbf{r}_2|} = \sum_{k=0}^{\infty}2\frac{2k+1}{c}\sum_{m=0}^{k}(-)^m(2-\delta_{m0})\frac{(k-m)!^2}{(k+m)!^2} \times P_k^m(\bar{\xi}_1)P_k^m(\bar{\eta}_1)Q_k^m(\bar{\xi}_2)P_k^m(\bar{\eta}_2)\cos m(\phi_1-\phi_2). \tag{C15}$$

We can write a similar expansion with spherical solid harmonics [7] when $r_1 < r_2$,

$$\frac{1}{|\mathbf{r}_1-\mathbf{r}_2|} = \sum_{n=0}^{\infty}\frac{r_1^n}{r_2^{n+1}}\sum_{m=0}^{n}(2-\delta_{m0})\frac{(n-m)!}{(n+m)!} \times P_n^m(\cos\theta_1)P_n^m(\cos\theta_2)\cos m(\phi_1-\phi_2), \tag{C16}$$

where (r_1,θ_1,ϕ_1) and (r_2,θ_2,ϕ_2) are the spherical coordinates of $\mathbf{r}_1$ and $\mathbf{r}_2$. We then substitute Eq. (C3) for $\mathbf{r_1}$ into Eq. (C15) to express it as an expansion on the same spherical harmonics basis,

$$\begin{aligned}\frac{1}{|\mathbf{r}_1-\mathbf{r}_2|} &= \sum_{k=0}^{\infty}2\frac{2k+1}{c}\sum_{m=0}^{k}(-)^m(2-\delta_{m0})\frac{(k-m)!^2}{(k+m)!^2}\left[\frac{(k+m)!}{(k-m)!}\sum_{n=m}^{k}\frac{(-)^{k+n}}{n!(n+m)!}\frac{(k+n)!}{(k-n)!}\frac{r_1^n}{c^n}P_n^m(\cos\theta_1)\right]Q_k^m(\bar{\xi}_2)P_k^m(\bar{\eta}_2)\cos m(\phi_1-\phi_2)\\ &= \sum_{n=0}^{\infty}\sum_{m=0}^{n}\sum_{k=n}^{\infty}2\frac{2k+1}{c}(2-\delta_{m0})\frac{(-)^{n+k+m}(k+n)!}{(k-n)!n!(n+m)!}\frac{(k-m)!}{(k+m)!}\frac{r_1^n}{c^n}P_n^m(\cos\theta_1)Q_k^m(\bar{\xi}_2)P_k^m(\bar{\eta}_2)\cos m(\phi_1-\phi_2),\end{aligned} \tag{C17}$$

where we have swapped the order of the sums, first $\sum_{m=0}^{k}\sum_{n=m}^{k} = \sum_{n=0}^{k}\sum_{m=0}^{n}$ and then $\sum_{k=0}^{\infty}\sum_{n=0}^{k} = \sum_{n=0}^{\infty}\sum_{k=n}^{\infty}$.

Because the functions $r_1^n P_n^m(\cos\theta_1)\cos m(\phi_1-\phi_2)$ are linearly independent, we can equate all terms with same n and m in Eqs. (C16) and (C17) to obtain Eq. (C4). This expansion is valid everywhere except on the line segment between the foci at $z = 0$ and $z = c$. ■

APPENDIX D: SIMPLIFICATION OF COEFFICIENTS c_n—PROOF OF EQ. (17)

We recall the definition of c_n [Eq. (16)] for $n \geqslant 0$:

$$c_n = \sum_{k=0}^{n} \frac{(-)^{n+k}}{k(\epsilon+1)+1} \frac{(n+k)!}{(n-k)!k!^2}$$
$$= \mu \sum_{k=0}^{n} \frac{(-)^{n+k}}{k+\mu} \frac{(n+k)!}{(n-k)!k!^2} \quad \text{with } \mu = \frac{1}{\epsilon+1}. \tag{D1}$$

We want to prove that

$$\sum_{k=0}^{n} \frac{(-)^k}{k+\mu} \frac{(n+k)!}{(n-k)!k!^2} = \frac{(-)^n}{\mu} \prod_{k=0}^{n} \frac{\mu-k}{\mu+k} = \frac{(1-\mu)(2-\mu)\cdots(n-\mu)}{\mu(\mu+1)(\mu+2)\cdots(\mu+n)} \tag{D2}$$

for a general μ. We first convert the left-hand side into a single fraction:

$$\frac{c_n}{\mu} = \frac{1}{\mu} - \frac{(n+1)n}{\mu+1} + \frac{(n+2)(n+1)n(n-1)}{(\mu+2)2!^2} - \frac{(n+3)(n+2)(n+1)n(n-1)(n-2)}{(\mu+3)3!^2} + \cdots + (-)^n \frac{2n(2n-1)\cdots 1}{(\mu+n)n!^2}$$
$$= \frac{(\mu+1)\cdots(\mu+n) - (n+1)n\alpha(\mu+2)(\mu+3)\cdots(\mu+n) + \frac{1}{2!^2}(n+2)(n+1)n(n-1)\mu(\mu+1)(\mu+3)\cdots(\mu+n) - \cdots}{\mu(\mu+1)(\mu+2)\cdots(\mu+n)}.$$

Both sides of Eq. (D2) are then fractions with the same denominator $\mu(\mu+1)(\mu+2)\cdots(\mu+n)$, and their numerators are polynomials of μ of degree n. These will be equal if they are equal at $n+1$ different points. Define $f(\mu)$ as the left-hand side numerator and $g(\mu)$ as the right-hand side numerator. Choose the $n+1$ points to be at $\mu = -q$, where $q = 0,1,2,\ldots n$. For $g(\mu)$ it is easy to show that

$$g(-q) = (1+q)(2+q)\cdots(n+q) = \frac{(n+q)!}{q!}.$$

For $f(\mu)$, note that it is composed of a sum of terms of the form $[(-)^b/b!^2]\mu(\mu+1)\cdots(\mu+b-1)(\mu+b+1)\cdots(\mu+n) \times (n+b)(n+b-1)\cdots(n-b+1)$ for some $b \in \{0,1,\ldots,n\}$. Setting $\mu = -q$, all terms vanish except the $(q+1)$th one. This term is

$$f(-q) = (-)^q \frac{1}{q!^2}(n+q)(n+q-1)\cdots(n-q+1)$$
$$\times (-q)(-q-1)\cdots(-) \times (1)(2)\cdots(n-q)$$
$$= \frac{(n+q)!}{q!}.$$

This applies to all $n+1$ values of q, so $f(\mu) = g(\mu)$, which proves Eqs. (D2) and (17). ■

APPENDIX E: PERPENDICULAR DIPOLE NEAR A SPHERE

1. Standard solution in spherical coordinates

We consider a dipole $\mathbf{p} = p\hat{\mathbf{z}}$ located at $\mathbf{R}_P$, on the z axis at a distance d from a sphere centered at the origin (i.e., $|\mathbf{R}_P| = R = a + d$). For convenience, the dimensionless potential $\bar{V}_\perp(\mathbf{r})$ is defined as $V_\perp = \bar{V}_\perp p/(4\pi\epsilon_0\epsilon_1 a R_P)$. The standard solution of this problem consists of expanding the dipole potential $\bar{V}_{\text{dip}-\perp}$ as a series of regular solid harmonics centered at the origin:

$$\bar{V}_{\text{dip}-\perp} = a R_P \frac{z - R_P}{|\mathbf{r} - R_P\hat{\mathbf{z}}|^3}$$
$$= -\frac{a}{R_P} \sum_{n=0}^{\infty} (n+1) \left(\frac{r}{R_P}\right)^n P_n(\cos\theta) \quad (r < R_P). \tag{E1}$$

The potential outside the sphere is $\bar{V}_{\text{out}-\perp} = \bar{V}_{\text{dip}-\perp} + \bar{V}_\perp$ with the reflected potential $\bar{V}_\perp(\mathbf{r})$ [2],

$$\bar{V}_\perp = \sum_{n=1}^{\infty} (n+1)\beta_n \left(\frac{R_I}{r}\right)^{n+1} P_n(\cos\theta), \tag{E2}$$

where β_n are the adimensional sphere polarizabilities defined in Eq. (3).

The electrostatic field derived from this potential can be used to calculate the quasistatic limit of the decay rate of a radiating dipole. It can be obtained from

$$\mathbf{E}_\perp(\mathbf{r}) = -\boldsymbol{\nabla} V_\perp = -\frac{\partial V_\perp}{\partial r}\hat{\mathbf{r}} - \frac{1}{r}\frac{\partial V_\perp}{\partial \theta}\hat{\boldsymbol{\theta}} - \frac{1}{r\sin\theta}\frac{\partial V_\perp}{\partial \phi}\hat{\boldsymbol{\phi}}. \tag{E3}$$

This gives

$$\mathbf{E}_\perp = E_0 \sum_{n=1}^{\infty} (n+1)\beta_n \left(\frac{a^2}{R_P r}\right)^{n+2}$$
$$\times \left\{(n+1)P_n(\cos\theta)\hat{\mathbf{r}} - \frac{d}{d\theta}[P_n(\cos\theta)]\hat{\boldsymbol{\theta}}\right\}, \tag{E4}$$
$$\text{with} \quad E_0 = \frac{p}{4\pi\epsilon_0\epsilon_1 a^3}.$$

The self-field at the dipole position ($r = R_P, \theta = 0$) is then

$$\mathbf{E}_{\text{sf}-\perp} = E_0 \sum_{n=1}^{\infty} (n+1)^2 \beta_n \left(\frac{a^2}{R_P^2}\right)^{n+2} \hat{\mathbf{z}}. \tag{E5}$$

From this, we can use Eq. (21) to deduce the modified decay rate in the electrostatics approximation [4,5]:

$$\frac{\Gamma_\perp}{\Gamma_0} = 1 + \frac{3}{2(k_1 a)^3}\sum_{n=1}(n+1)^2 \mathrm{Im}(\beta_n)\left(\frac{a^2}{R_P^2}\right)^{n+2}. \quad \text{(E6)}$$

Like with the point charge, we want to improve the rate of convergence of these series by extracting image terms and then reformulating the expansion in terms of spheroidal harmonics.

2. Analytic expressions for image sources

We start from the reflected potential for a perpendicular dipole given in Eq. (E2). Writing β_n explicitly, it can be rewritten as

$$\bar{V}_\perp = (\epsilon - 1)\sum_{n=0}^{\infty} \frac{n(n+1)}{n(\epsilon+1)+1}\left(\frac{R_I}{r}\right)^{n+1} P_n(\cos\theta). \quad \text{(E7)}$$

We then isolate the first two dominant terms in the fraction (as $n \to \infty$):

$$\frac{n(n+1)}{n(\epsilon+1)+1} = \frac{n}{\epsilon+1} + \frac{\epsilon}{(\epsilon+1)^2} - \frac{\epsilon}{(\epsilon+1)^2[n(\epsilon+1)+1]}. \quad \text{(E8)}$$

The sum over the second term on the right-hand side in Eq. (E8) is the same as found for the point charge [Eq. (6)]. It can be evaluated analytically and corresponds to the potential created by an image point charge located at I.

A similar expression exists for the sum over the first term. It can be obtained by differentiating Eq. (6) with respect to z. First note that for $n \geqslant 0$

$$\frac{\partial}{\partial z}\frac{P_n(\cos\theta)}{r^{n+1}} = -(n+1)\frac{P_{n+1}(\cos\theta)}{r^{n+2}}. \quad \text{(E9)}$$

Then by applying $R_I\partial_z$ to both sides of Eq. (6) and reindexing the sum from n to $n-1$ we obtain

$$\sum_{n=0}^{\infty} n\left(\frac{R_I}{r}\right)^{n+1} P_n(\cos\theta) = \left(\frac{R_I}{r'}\right)^2 \cos\theta' = R_I^2\frac{z'}{r'^3}, \quad \text{(E10)}$$

which is proportional to the potential of an image dipole located at I oriented along z [7] and provides an analytic expression for the sum over the first term on the right-hand side of Eq. (E8). By substituting Eq. (E8) into Eq. (E7) and using the analytic forms of the series given in Eqs. (6) and (E10), we obtain

$$\bar{V}_\perp = \beta_\infty\frac{R_I^2 z'}{r'^3} + \frac{\epsilon\beta_\infty}{\epsilon+1}\frac{R_I}{r'} - \frac{\epsilon\beta_\infty}{(\epsilon+1)}\sum_{n=0}^{\infty}\frac{1}{n(\epsilon+1)+1}\left(\frac{R_I}{r}\right)^{n+1} P_n(\cos\theta). \quad \text{(E11)}$$

The same approach can be followed to obtain the next image source by splitting off the next leading order [$1/(n+1)$ dependence] of β_n. In fact, this term is the same logarithmic source that was obtained for the point charge. Because it is singular on the segment OI, we do not separate it and include it in the expansion in terms of spheroidal harmonics.

3. New approach with spheroidal harmonics

Following the same logic as in Sec. III for a point charge, we search for an equivalent solution where we keep the image point source terms (there are two of them here) and express the rest as a spheroidal solid harmonics expansion:

$$\bar{V}_\perp = R_I^2\beta_\infty\frac{z'}{r'^3} + \frac{\epsilon\beta_\infty}{\epsilon+1}\frac{R_I}{r'} + \sum_{n=0} d_n Q_n(\bar{\xi})P_n(\bar{\eta}). \quad \text{(E12)}$$

The coefficients d_n are again obtained by substituting Eq. (12) into the series in Eq. (E11) and swapping the order of the sums,

$$d_n = -\beta_\infty\frac{\epsilon}{\epsilon+1}2(2n+1)\sum_{k=0}^{n}\frac{(-1)^{n+k}}{k(\epsilon+1)+1}\frac{(n+k)!}{k!^2(n-k)!} = -\beta_\infty\frac{\epsilon}{\epsilon+1}2(2n+1)c_n, \quad \text{(E13)}$$

where c_n has been defined in Eqs. (16) and (17).

The new potential solution then takes the form

$$\bar{V}_\perp = \beta_\infty R_I^2\frac{z'}{r'^3} + \frac{\epsilon\beta_\infty}{\epsilon+1}\frac{R_I}{r'} - 2\frac{\epsilon\beta_\infty}{\epsilon+1}\sum_{n=0}^{\infty}(2n+1)c_n Q_n(\bar{\xi})P_n(\bar{\eta}). \quad \text{(E14)}$$

4. Electric field and modified decay rate with new formulation

From this latest expression, we can deduce a faster converging form of the electric field in terms of spheroidal harmonics. Note that multiple coordinates can be used (r, θ, r', θ', $\bar{\xi}$, $\bar{\eta}$) to express the field in a more compact form:

$$\mathbf{E}_\perp = E_0\beta_\infty\left\{\left(2\frac{R_I^3}{r'^3}\cos\theta - 3\frac{R_I^4 r}{r'^5}\sin^2\theta\right) - \frac{\epsilon}{\epsilon+1}\frac{R_I^2}{r'^3}(R_I\cos\theta - r) - \frac{2\epsilon}{\epsilon+1}\frac{R_I}{r}\sum_{n=0}^{\infty}(2n+1)(n+1)c_n \times\left[Q_n(\bar{\xi})P_n(\bar{\eta}) + \frac{Q_n(\bar{\xi})P_{n+1}(\bar{\eta}) - Q_{n+1}(\bar{\xi})P_n(\bar{\eta})}{\bar{\xi}-\bar{\eta}}\right]\right\}\hat{\mathbf{r}} + E_0\beta_\infty\sin\theta\left(\frac{R_I^3(r^2 + R_I z - 2R_I^2)}{r'^5} + \frac{\epsilon}{\epsilon+1}\frac{R_I^3}{r'^3} - \frac{2\epsilon}{\epsilon+1}\frac{R_I}{r}\sin\theta\sum_{n=0}^{\infty}(2n+1)(n+1)c_n\left\{\frac{Q_n(\bar{\xi})P_n(\bar{\eta})\cos\theta}{\sin^2\theta} + \frac{r}{r'}\left[\frac{Q_n(\bar{\xi})P_{n+1}(\bar{\eta})}{\bar{\eta}^2-1} - \frac{Q_{n+1}(\bar{\xi})P_n(\bar{\eta})}{\bar{\xi}^2-1}\right]\right\}\right)\hat{\boldsymbol{\theta}}. \quad \text{(E15)}$$

The self-field $\boldsymbol{E}_{\mathrm{sf}-\perp}$ is then obtained by evaluating Eq. (E15) at the dipole position, whose coordinates are

$$\begin{aligned} r &= R_P, & \theta &= 0, \\ r' &= R_P - R_I = R_I\delta_P, & \theta' &= 0, \\ \bar{\xi} &= \bar{\xi}_P = 2\frac{R_P^2}{a^2} - 1 = 1 + 2\delta_P, & \bar{\eta} &= 1, \end{aligned}$$

$$\text{where } \delta_P = \frac{R_P^2}{a^2} - 1.$$

Note that the adimensional parameter $\delta_P > 0$ becomes small when the dipole is close to the surface. From $\boldsymbol{E}_{\mathrm{sf}-\perp}$, we then deduce the expression for the modified decay rate given in Eq. (21).

APPENDIX F: PARALLEL DIPOLE NEAR A SPHERE

In this section, we adapt the derivations presented for the perpendicular dipole to the case of a parallel dipole. The main difference is that all spherical and spheroidal harmonic expansions now contain Legendre functions P_n^m, Q_n^m, with $m = 1$, instead of $m = 0$ for perpendicular dipoles.

1. Solution in spherical coordinates

The standard solution of this problem consists of expanding the dipole potential as a series of regular solid harmonics centered at the origin. For a dipole along x, located on the z axis at $z = R_P$, we have [analogous to Eq. (E1)]

$$\begin{aligned} \bar{V}_{\mathrm{dip}-\parallel} &= \frac{aR_P x}{|\mathbf{r} - R_P\hat{\mathbf{z}}|^3} \\ &= \frac{a}{R_P}\sum_{n=1}^{\infty}\left(\frac{r}{R_P}\right)^n P_n^1(\cos\theta)\cos\phi \quad (r < R_P). \end{aligned} \tag{F1}$$

The solution of the problem outside the sphere ($r > a$) is then given by $\bar{V}_{\mathrm{out}-||} = \bar{V}_{\mathrm{dip}-\parallel} + \bar{V}_{\parallel}$, with the reflected potential $\bar{V}_{\parallel}$ given by [2]

$$\bar{V}_{\parallel} = -\sum_{n=1}^{\infty}\beta_n\left(\frac{R_I}{r}\right)^{n+1} P_n^1(\cos\theta)\cos\phi, \tag{F2}$$

where β_n are the adimensional sphere polarizabilities as defined in Eq. (3).

The reflected electric field outside the sphere is then

$$\begin{aligned} \mathbf{E}_{\parallel} = E_0\sum_{n=1}^{\infty}\beta_n\left(\frac{R_I}{r}\right)^{n+2}\Bigg\{ &-(n+1)P_n^1(\cos\theta)\cos\phi\hat{\mathbf{r}} \\ &+\frac{d}{d\theta}\left[P_n^1(\cos\theta)\right]\cos\phi\hat{\boldsymbol{\theta}} - \frac{P_n^1(\cos\theta)}{\sin\theta}\sin\phi\hat{\boldsymbol{\phi}}\Bigg\}, \end{aligned} \tag{F3}$$

where $E_0 = p/(4\pi\epsilon_0\epsilon_1 a^3)$. To calculate the self-field $E_{\mathrm{sf}-\parallel}$ (at $r = R_P$, $\theta = 0$), we need to take the limit as $\theta \to 0$. We use the equalities

$$\begin{aligned} &P_n^1(1) = 0, \\ &\lim_{\theta\to 0}\left\{\frac{d}{d\theta}\left[P_n^1(\cos\theta)\right]\right\} = \lim_{\theta\to 0}\left[\frac{P_n^1(\cos\theta)}{\sin\theta}\right] = \frac{n(n+1)}{2}, \end{aligned} \tag{F4}$$

and

$$\hat{\mathbf{x}} = \sin\theta\cos\phi\hat{\mathbf{r}} + \cos\theta\cos\phi\hat{\boldsymbol{\theta}} - \sin\phi\hat{\boldsymbol{\phi}} \tag{F5}$$

to obtain

$$\mathbf{E}_{\mathrm{sf}-\parallel} = E_0\sum_{n=1}^{\infty}\frac{n(n+1)}{2}\beta_n\left(\frac{a^2}{R_P^2}\right)^{n+2}\hat{\mathbf{x}}. \tag{F6}$$

The modified decay rate is therefore

$$\frac{\Gamma_{\parallel}}{\Gamma_0} = 1 + \frac{3}{4(k_1 a)^3}\sum_{n=1}^{\infty} n(n+1)\mathrm{Im}(\beta_n)\left(\frac{a^2}{R_P^2}\right)^{n+2}. \tag{F7}$$

2. Analytic expressions for image terms

We now come back to the potential [Eq. (F2)]. Following the same arguments as for the perpendicular dipole, one can recognize closed-form expressions for the first few dominant terms. β_n can be split and analytic expressions for the series can be identified. Explicitly,

$$\frac{n}{n(\epsilon+1)+1} = \frac{1}{\epsilon+1} - \frac{1}{(\epsilon+1)^2}\left\{\frac{1}{n} + \frac{1}{n[n(\epsilon+1)+1]}\right\}. \tag{F8}$$

The first term results in the series

$$\sum_{n=1}^{\infty}\left(\frac{R_I}{r}\right)^{n+1} P_n^1(\cos\theta)\cos\phi = R_I^2\frac{x'}{r'^3}, \tag{F9}$$

where we have recognized the expansion of a dipole offset along the z axis (and located at $z = R_I$). This is the image dipole, whose orientation is in this case opposite to the real dipole.

The second term gives the series

$$\sum_{n=1}^{\infty}\frac{1}{n}\left(\frac{R_I}{r}\right)^{n+1} P_n^1(\cos\theta)\cos\phi. \tag{F10}$$

In contrast with the case of a perpendicular dipole where an image point charge was identified, it is not straightforward here to recognize an analytic expression. To develop this further, we will use (for $n \geqslant 1$)

$$P_n^1(\cos\theta) = \frac{n}{\sin\theta}[-\cos\theta P_n(\cos\theta) + P_{n-1}(\cos\theta)]. \tag{F11}$$

We then have

$$\begin{aligned} &\sum_{n=1}^{\infty}\frac{1}{n}\left(\frac{R_I}{r}\right)^{n+1} P_n^1(\cos\theta)\cos\phi \\ &= \frac{\cos\phi}{\sin\theta}\sum_{n=1}^{\infty}\left(\frac{R_I}{r}\right)^{n+1}(P_{n-1} - \cos\theta P_n) \\ &= \frac{\cos\phi}{\sin\theta}\left[\frac{R_I}{r}\sum_{n=0}^{\infty}\left(\frac{R_I}{r}\right)^{n+1} P_n - \cos\theta\sum_{n=1}^{\infty}\left(\frac{R_I}{r}\right)^{n+1} P_n\right] \\ &= \frac{\cos\phi}{\sin\theta}\left[\frac{R_I}{r}\frac{R_I}{r'} - \cos\theta\left(\frac{R_I}{r'} - \frac{R_I}{r}\right)\right] \quad \text{using Eq. (6)} \\ &= \frac{R_I\cos\phi}{r\sin\theta}(\cos\theta - \cos\theta') \quad \text{since } \cos\theta' = \frac{r\cos\theta - R_I}{r'} \\ &= \frac{R_I x}{\rho^2}(\cos\theta - \cos\theta'). \end{aligned} \tag{F12}$$

Note that the above expression is singular on the line from O to I, but converges to a finite value elsewhere even on the z axis.

Putting those results together, and using $x' = x$, we have for the potential

$$\bar{V}_{\parallel} = -\beta_\infty \frac{R_I^2 x}{r'^3} - \frac{\beta_\infty}{\epsilon+1}\frac{R_I x(\cos\theta' - \cos\theta)}{r^2 \sin^2\theta} - \frac{\beta_\infty \cos\phi}{\epsilon+1}\sum_{n=1}^{\infty}\left(\frac{R_I}{r}\right)^{n+1}\frac{P_n^1(\cos\theta)}{n[n(\epsilon+1)+1]}. \quad \text{(F13)}$$

3. New approach with spheroidal harmonics

The main difference with the perpendicular dipole is that only the first dominant analytic term in the expression above is a point singularity. Since the second term exhibits the line singularity from O to I, there is no reason to isolate it when looking for the expansion in spheroidal harmonics. We therefore start from the potential with the image dipole term only, namely,

$$\bar{V}_{\parallel} = -\beta_\infty \frac{R_I^2 x}{r'^3} + \beta_\infty \cos\phi \sum_{n=1}^{\infty}\left(\frac{R_I}{r}\right)^{n+1}\frac{P_n^1(\cos\theta)}{n(\epsilon+1)+1}. \quad \text{(F14)}$$

This can then be converted into a spheroidal solid harmonics expansion using Eq. (C4) for $m = 1$, which reads

$$\left(\frac{R_I}{r}\right)^{n+1} P_n^1(\cos\theta) = -2\sum_{k=n}^{\infty}\frac{(-)^{n+k}}{n!(n-1)!}\frac{(k+n)!}{(k-n)!} \times \frac{2k+1}{k(k+1)} Q_k^1(\bar{\xi}) P_k^1(\bar{\eta}). \quad \text{(F15)}$$

The series in the previous equation for $\bar{V}_{\parallel}$ then reads

$$\sum_{n=1}^{\infty}\left(\frac{R_I}{r}\right)^{n+1}\frac{P_n^1(\cos\theta)}{n(\epsilon+1)+1} = -2\sum_{n=1}^{\infty}\frac{2n+1}{n(n+1)}\sum_{k=1}^{n}\frac{(-)^{n+k}k}{k\epsilon+k+1}\frac{(n+k)!}{k!^2(n-k)!}Q_n^1(\bar{\xi})P_n^1(\bar{\eta}). \quad \text{(F16)}$$

Here the order of summation was swapped then the indices relabeled ($n \leftrightarrow k$).

Using the decomposition

$$(\epsilon+1)\frac{k}{k\epsilon+k+1} + \frac{1}{k\epsilon+k+1} = 1, \quad \text{(F17)}$$

we also obtain the following relation:

$$(\epsilon+1)\sum_{k=0}^{n}\frac{(-)^{n+k}k}{k(\epsilon+1)+1}\frac{(n+k)!}{k!^2!(n-k)!} + \sum_{k=0}^{n}\frac{(-)^{n+k}}{k(\epsilon+1)+1}\frac{(n+k)!}{k!^2(n-k)!} = \sum_{k=0}^{n}\frac{(-)^{n+k}(n+k)!}{k!^2(n-k)!} = 1. \quad \text{(F18)}$$

The latter equality can be obtained by evaluating Eq. (C3) at $m = 0$, $\bar{\xi} = \bar{\eta} = 1$. The second term above can be identified as c_n [Eq. (16)] and the sum in the first term can start at $k = 1$ without affecting the result, so we deduce

$$\sum_{k=1}^{n}\frac{(-)^{n+k}k}{k\epsilon+k+1}\frac{(n+k)!}{k!^2!(n-k)!} = \frac{1-c_n}{\epsilon+1}. \quad \text{(F19)}$$

The potential, therefore, takes the form

$$\bar{V}_{\parallel} = -\beta_\infty \frac{R_I^2 x}{r'^3} + \frac{2\beta_\infty}{\epsilon+1}\cos\phi\sum_{n=1}^{\infty}\frac{2n+1}{n(n+1)}(c_n-1)Q_n^1(\bar{\xi})P_n^1(\bar{\eta}). \quad \text{(F20)}$$

4. Electric field and modified decay rate with new approach

Starting from the proposed new formula for the potential solution [Eq. (F20)], we can deduce the electric field in terms of the more convergent spheroidal harmonics expansions:

$$\begin{aligned}\mathbf{E}_{\parallel} = &-E_0\cos\phi\beta_\infty\left\{\frac{R_I^3\sin\theta(2r^2 - R_I z - R_I^2)}{r'^5} - \frac{2}{\epsilon+1}\frac{R_I}{r}\sum_{n=1}^{\infty}(2n+1)(c_n-1)\right.\\ &\left.\times\left[\frac{Q_n^1(\bar{\xi})P_n^1(\bar{\eta})}{n} + \frac{Q_n^1(\bar{\xi})P_{n+1}^1(\bar{\eta}) - Q_{n+1}^1(\bar{\xi})P_n^1(\bar{\eta})}{(n+1)(\bar{\xi}-\bar{\eta})}\right]\right\}\hat{\mathbf{r}} - E_0\cos\phi\beta_\infty\left\{\frac{R_I^3}{r'^5}\left(r'^2\cos\theta - 3R_I r\sin^2\theta\right)\right.\\ &\left.+\frac{2}{\epsilon+1}\frac{R_I}{r\sin\theta}\sum_{n=1}^{\infty}(2n+1)(c_n-1)\left[\frac{Q_n^1(\bar{\xi})P_n^1(\bar{\eta})}{n}\cos\theta - \frac{R_I^2}{4rr'}\frac{Q_n^1(\bar{\xi})P_{n+1}^1(\bar{\eta})(\bar{\xi}^2-1) - Q_{n+1}^1(\bar{\xi})P_n^1(\bar{\eta})(\bar{\eta}^2-1)}{(n+1)}\right]\right\}\hat{\boldsymbol{\theta}}\\ &-E_0\sin\phi\beta_\infty\left[\frac{R_I^3}{r'^3} - \frac{2}{\epsilon+1}\frac{R_I}{r\sin\theta}\sum_{n=1}^{\infty}\frac{2n+1}{n(n+1)}(c_n-1)Q_n^1(\bar{\xi})P_n^1(\bar{\eta})\right]\hat{\boldsymbol{\phi}}. \quad \text{(F21)}\end{aligned}$$

To calculate the self-field we substitute the dipole coordinates and take limits as $\theta \to 0$. Then we use Eq. (20) to obtain the modified decay rate for a parallel dipole given in Eq. (21).

[1] P. M. Morse and H. Feshbach, *Methods of Theoretical Physics* (McGraw-Hill, New York, 1953).

[2] J. A. Stratton, *Electromagnetic Theory* (McGraw-Hill, New York, 1941).

[3] G. Ford and W. Weber, Phys. Rep. **113**, 195 (1984).

[4] E. C. Le Ru and P. G. Etchegoin, *Principles of Surface-enhanced Raman Spectroscopy and Related Plasmonic Effects* (Elsevier, Amsterdam, 2009).

[5] A. Moroz, J. Phys. Chem. C **115**, 19546 (2011).

[6] I. V. Lindell, Radio Sci. **27**, 1 (1992).

[7] J. D. Jackson, *Classical Electrodynamics*, 2nd ed. (Wiley, New York, 1998).

[8] M. Abramowitz and I. A. Stegun (eds.), *Handbook of Mathematical Functions* (Dover, New York, 1972).

[9] G. Jansen, J. Phys. A: Math. Gen. **33**, 1375 (2000).

[10] V. A. Antonov and A. S. Baranov, Tech. Phys. **47**, 80 (2002).

[11] B. I. Schneider, J. Segura, A. Gil, X. Guan, and K. Bartschat, Comp. Phys. Commun. **181**, 2091 (2010).

[12] F. T. Ladani, S. Campione, C. Guclu, and F. Capolino, Phys. Rev. B **90**, 125127 (2014).

[13] M. Sukharev, N. Freifeld, and A. Nitzan, J. Phys. Chem. C **118**, 10545 (2014).

[14] R. R. Chance, A. Prock, and R. Silbey, Adv. Chem. Phys. **37**, 1 (1978).

[15] S. M. Barnett, B. Huttner, and R. Loudon, Phys. Rev. Lett. **68**, 3698 (1992).

[16] L. Novotny and B. Hecht, *Principles of Nano-optics* (Cambridge University Press, Cambridge, U.K., 2006).

[17] P. G. Etchegoin, E. C. Le Ru, and M. Meyer, J. Chem. Phys. **125**, 164705 (2006).

[18] L. Li, X.-K. Kang, and M.-S. Leong, *Spheroidal Wave Functions in Electromagnetic Theory* (Wiley, New York, 2002).